



**Manchester
Metropolitan
University**

Borges, Joana, Higginbottom, Thomas P, Cain, Bradley, Gadiye, Donatus E, Kisingo, Alex, Jones, Martin ORCID logoORCID: <https://orcid.org/0000-0002-2510-8697> and Symeonakis, Elias ORCID logoORCID: <https://orcid.org/0000-0003-1724-2869> (2022) Landsat time series reveal forest loss and woody encroachment in the Ngorongoro Conservation Area, Tanzania. *Remote Sensing in Ecology and Conservation*. ISSN 2056-3485

Downloaded from: <https://e-space.mmu.ac.uk/629953/>

Version: Published Version

Publisher: Wiley Open Access

DOI: <https://doi.org/10.1002/rse2.277>


Usage rights: Creative Commons: Attribution-Noncommercial 4.0

Please cite the published version

<https://e-space.mmu.ac.uk>

ORIGINAL RESEARCH

Landsat time series reveal forest loss and woody encroachment in the Ngorongoro Conservation Area, Tanzania

Joana Borges¹ , Thomas P. Higginbottom², Bradley Cain¹, Donatus E. Gadiye³, Alex Kisingo⁴, Martin Jones¹ & Elias Symeonakis¹

¹Department of Natural Sciences, Manchester Metropolitan University, Manchester M15 6BH, UK

²School of GeoSciences, University of Edinburgh, Edinburgh EH9 3FF, UK

³Ngorongoro Conservation Area, Arusha, Tanzania

⁴College of African Wildlife Management, Mweka, Kibosho Magharibi, Tanzania

Keywords

BFAST, EnMAP, land cover change, Landsat, linear trend, Ngorongoro Conservation Area, regression-based unmixing, time series

Correspondence

Elias Symeonakis, Department of Natural Sciences, Manchester Metropolitan University, Manchester M15 6BH, UK. Tel: +44 (0)161 2471587; E-mail: e.symeonakis@mmu.ac.uk

Editor: Mat Disney

Associate Editor: Shaun Leveck

Received: 15 September 2021; Revised: 31 March 2022; Accepted: 8 May 2022

doi: 10.1002/rse2.277

Abstract

The Ngorongoro Conservation Area (NCA) of Tanzania, is globally significant for biodiversity conservation due to the presence of iconic fauna, and, since 1959 has been managed as a unique multiple land-use areas to mutually benefit wildlife and indigenous residents. Understating vegetation dynamics and ongoing land cover change processes in protected areas is important to protect biodiversity and ensure sustainable development. However, land cover changes in savannahs are especially difficult, as changes are often long-term and subtle. Here, we demonstrate a Landsat-based monitoring strategy incorporating (i) regression-based unmixing for the accurate mapping of the fraction of the different land cover types, and (ii) a combination of linear regression and the BFAST trend break analysis technique for mapping and quantifying land cover changes. Using Google Earth Pro and the EnMap-Box software, the fractional cover of the main land cover types of the NCA were accurately mapped for the first time, namely bareland, bushland, cropland, forest, grassland, montane heath, shrubland, water and woodland. Our results show that the main changes occurring in the NCA are the degradation of upland forests into bushland: we exemplify this with a case study in the Lerai Forest; and found declines in grassland and co-incident increases in shrubland in the Serengeti Plains, suggesting woody encroachment. These changes threaten the wellbeing of livestock, the livelihoods of resident pastoralists and of the wildlife dependent on these grazing areas. Some of the land cover changes may be occurring naturally and caused by herbivory, rainfall patterns and vegetation succession, but many are linked to human activity, specifically, management policies, tourism development and the increase in human population and livestock. Our study provides for the first time much needed and highly accurate information on long-term land cover changes in the NCA that can support the sustainable management and conservation of this unique UNESCO World Heritage Site.

Introduction

African savannah environments provide essential ecosystem services to communities, sustain endemic biodiversity and play a critical role in regulating carbon cycles (Liu et al., 2015; McNicol et al., 2018; Poulter et al., 2014; Schneibel et al., 2017). In recent years, the provision of

ecosystem services from many savannah regions has progressively declined due to agricultural expansion, woodland degradation, invasive species, bush encroachment, climate change and management policies, all of which can place wildlife and communities at risk (Schneibel et al., 2017; Symeonakis & Higginbottom, 2014; Tsalyuk et al., 2017).

The Ngorongoro Conservation Area (NCA) in Northern Tanzania is a designated United Nations Educational, Scientific and Cultural Organisation (UNESCO) World Heritage Site for exceptional natural and cultural values (UNESCO, 2010). It is part of the world's largest intact savannah systems, the Greater Serengeti Ecosystem, which includes the Serengeti National Park and the Maasai Mara, where one of Africa's largest animal migrations takes place (Masao et al., 2015; Swanson, 2007). The NCA also supports the largest population of the critically endangered Eastern Black Rhinoceros *Diceros bicornis michaeli* in Tanzania (Amiyo, 2006; Goddard, 1968; Mills et al., 2006). The density and diversity of wildlife in the NCA is of global importance for biodiversity conservation and economically important for Tanzania. For instance, in 2016 over 1 million tourists visited the NCA, generating revenue of approximately \$70 million (Slootweg, 2016, 2017). The NCA is also unique as it operates as a multiple land-use model designed to protect not only wildlife but also the lifestyle of the resident Maasai pastoralists (Niboye, 2010).

The NCA vegetation is composed of a combination of highland forests around the Ngorongoro Crater, savannah woodland and shortgrass plains (Herlocker & Dirschl, 1972). Over the last 50 years, African savannahs have undergone considerable land cover changes, including forest degradation, spread of invasive plant species, and woody encroachment (Amiyo, 2006; Higginbottom et al., 2018; Ludwig et al., 2019; Mills et al., 2006; Symeonakis et al., 2018; Venter et al., 2018). In the NCA highlands, forest degradation is of particular concern, as these forests provide ecosystem services to the Maasai through the provision of fuel wood, traditional medicinal plants, and forage for livestock (Swanson, 2007). Additionally, upland forests provide shelter for wildlife and regulate water resources (Swanson, 2007). Meanwhile, in the grassland plains, woody encroachment and invasive species can reduce rangeland carrying capacity, directly affecting wildlife and the Maasai livestock (Venter et al., 2018).

Land cover changes in the NCA are driven by a combination of local and global drivers (Homewood et al., 2001; Masao et al., 2015; Niboye, 2010). Firstly, the Maasai community within the NCA increased from roughly 8000 in 1959 to almost 100 000 in 2018, with an accompanying livestock population of approximately 800 000 in 2018 (Lyimo et al., 2020; Manzano & Yamat, 2018). Population growth has led to the expansion of settlements, livestock bomas and demand for water resources (TAWIRI & NCAA, 2020). In addition, tourism, grazing pressure, climate change and management decisions also seem to be contributors to change (Homewood et al., 2001; Masao et al., 2015; Niboye, 2010). Many of these changes have led to the

decline in habitat quality (Amiyo, 2006; Estes et al., 2006; Niboye, 2010). Less suitable habitats with limited opportunities for browsing and grazing encourage inter- and intraspecific competition for resources, threatening wildlife populations and their distribution, and subsequently raising concerns of biodiversity loss and increasing human-wildlife conflicts (Amiyo, 2006; Kija et al., 2020; Makacha et al., 1979; Niboye, 2010). In addition, for the Maasai pastoralists these changes threaten the quantity and quality of pasture resources for livestock and consequently food security. Previous small-scale studies have mentioned ongoing land cover changes within the NCA, but the large-scale dynamics remain poorly understood (Boone et al., 2006; Homewood et al., 2001; Masao et al., 2015). The research available for the NCA is mostly based on field surveys and aerial photography, which provide highly detailed information at the species level but do not offer large-scale, holistic coverage (Amiyo, 2006; Herlocker & Dirschl, 1972).

Over the last five decades, Earth-observation (EO) data have increasingly been used to map and monitor land cover (Adole et al., 2016; Woodcock et al., 2008; Wulder et al., 2012). In particular, the Landsat archive provides open-access, long-term data, with 30-metre spatial resolution and six spectral bands that are well suited for vegetation mapping. However, savannah landscapes are challenging to map due to their heterogeneous and complex characteristics, incorporating a mixture of woody vegetation (trees, bushes and shrubs), different grass species and bare land (Borges et al., 2020; Ludwig et al., 2019; Mathieu et al., 2013; Settle & Drake, 1993; Symeonakis et al., 2018; Venter et al., 2018). Mapping and monitoring change in savannah environments is even more challenging, as most changes occur gradually and incrementally, resulting in subtle spectral changes that are difficult to detect using imagery with a moderate spatial resolution. Recently, the combination of synthetically generated mixed samples with machine learning regression methods has proved effective for mapping fractional cover in complex environments (Okujeni et al., 2013; Senf et al., 2020; Suess et al., 2018). Meanwhile, the development of time-series methodologies has facilitated a more ecologically meaningful quantification of landscape change detection. These time-series approaches exploit the higher observation densities that are now available, to detect changes in either spectral bands, vegetation indices or derived layers such as class probabilities or fractional coverage. (Schneibel et al., 2017; Schwieder et al., 2016; Souverijns et al., 2020).

There is a pressing need to quantify the extent and magnitude of land cover changes within the NCA, to identify vulnerable areas and prevent potential threats to habitats and livelihoods. The NCA's multiple-use approach, which attempts to reconcile biodiversity

protection and the needs of local people, is a notoriously challenging task (Harris et al., 2020). Moreover, in the context of protected area management, an improved understanding of land cover dynamics is imperative for sustainable development, to support effective land use planning, conserve and manage biodiversity and ensure the long-term survival of wildlife and the prosperity of resident human communities.

The main aim of the paper is to support the sustainable management of the NCA by developing an Earth-observation-based approach for monitoring multi-faceted land cover changes occurring over the past 35 years. We employ the approach of Okujeni et al. (2013) to produce near-annual fractional cover maps for nine constituent land cover classes of the NCA. To identify the various change processes, we employ two pixel level time-series analyses. Firstly, we employ monotonic linear trend analysis to detect long-term changes in land cover (Herrmann et al., 2005; Higginbottom & Symeonakis, 2014). Secondly, we used the Breaks For Additive Season and Trend (BFAST) piece-wise linear regression method to detect possible breakpoints, specifically for upland forest cover (Grogan et al., 2016; Lewińska et al., 2020; Morrison et al., 2018; Schmidt et al., 2015; Wu et al., 2020). We use the linear trend analysis to detect long-term, incremental land cover changes, such as shrub encroachment and grassland decline. Meanwhile, BFAST is well-suited to identifying abrupt shifts and reversals in trends that may be obscured by monotonic analysis, such as deforestation and regrowth (Verbesselt, Hyndman, Zeileis, et al., 2010).

Study area

The NCA covers an area of around 8283 km² (Swanson, 2007, Fig. 1). It contains the largest, intact volcanic caldera in the Ngorongoro Crater and has highly abundant and diverse wildlife (Estes et al., 2006, Fig. 1C). Annual rainfall ranges from 450 mm/year in the lowlands to 1200 mm/year in the highlands (Boone et al., 2007; Fig. S1). Rainfall follows a bimodal pattern, characteristic of East Africa, comprising two wet seasons: the main between March and May, and a shorter one between November and December (Pellikka et al., 2018). During the dry season, temperature ranges between 11 and 20°C, while in the wet season it ranges between 7 and 15°C (Amiyo, 2006).

Materials and Methods

Landsat image acquisition and processing

We acquired and processed Landsat Collections Level 1 Tier 1 imagery from 1985 to 2020. Based on our previous

study, we selected images from the short dry season (January–April), which enables the highest separability of the land cover types (Borges et al., 2020). For the 35-year study period, we obtained 26 images with cloud cover less than 75%, acquisition dates ranged from 9 January to 28 April (Fig. 2). No suitable images were available for 1986, 1988, 1991–1994 and 1996–1999. The Landsat collections are pre-processed for atmospheric corrections using the Landsat Ecosystem Disturbance Adaptive Processing System (LEDAPS) routine (Masek et al., 2006). Cloud masking was provided by F-mask (Schmidt et al., 2013). We topographically corrected the images using a Sun Canopy Sensor (Gu & Gillespie, 1998) and C-correction approach (Teillet et al., 1982). The Normalised Difference Vegetation Index (NDVI; Tucker, 1979) was calculated using the standard equation and added to the spectral bands, NDVI is useful in savannahs that do not feature dense forest canopies (Prince & Tucker, 1986). We used the Google Earth Engine cloud-computing environment for all Landsat processing (Gorelick et al., 2017; Moore & Hansen, 2011).

Fractional cover mapping

Our approach focusses on the generation of near-annual fractional land cover maps, where each pixel represents the 0%–100% coverage of the constituent land cover types. The production of fractional land cover maps requires predictive models quantifying the relationship between the input satellite imagery products and the target classes as *fractions*. Previous studies have generated fractional training data by the manual interpretation or classification of imagery with a finer spatial resolution than the input predictive layers; however, this is a time-consuming exercise (Baumann et al., 2018). More recently, Okujeni et al. (2013) developed an approach to generate mixed samples from pure spectra representing 100% class coverage, producing synthetic samples of mixed fractions for the desired land cover types. This synthetic training data can be combined with modern machine learning models and has proved highly effective in a range of settings (Okujeni et al., 2013; Senf et al., 2020; Suess et al., 2018).

Here, we expand on the methodology developed by Okujeni et al. (2013). First, we developed a spectral library for a land cover schema of the NCA. We focussed on ecological meaningful land cover types comprised of mixed vegetation communities which are spectrally separable. Second, we generated synthetically mixed training data using the approach proposed by Okujeni et al. (2013). Finally, we input these synthetic samples into a Random Forest regression model. To guide our analysis, we employed a land cover map of the NCA

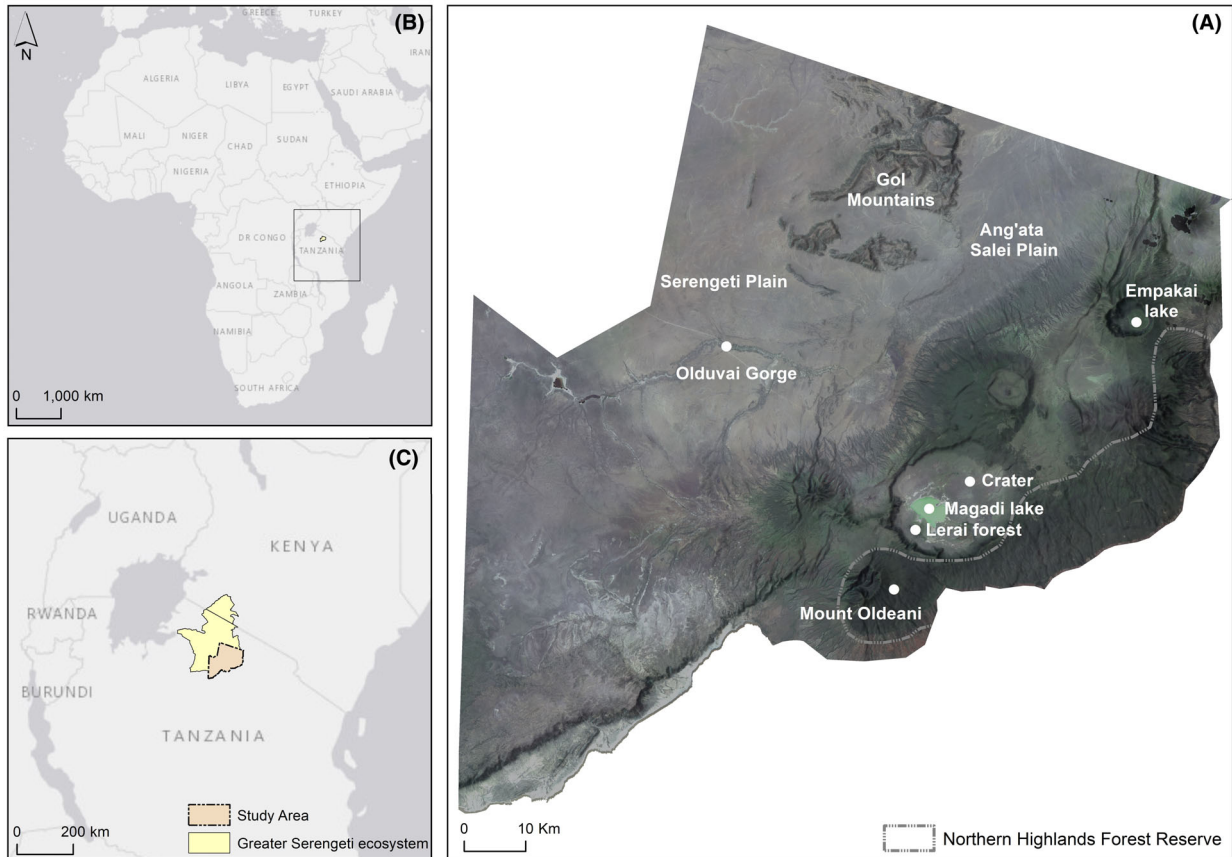


Figure 1. The Ngorongoro Conservation Area (A) and its location within Africa (B), Tanzania and the Greater Serengeti ecosystem (C).

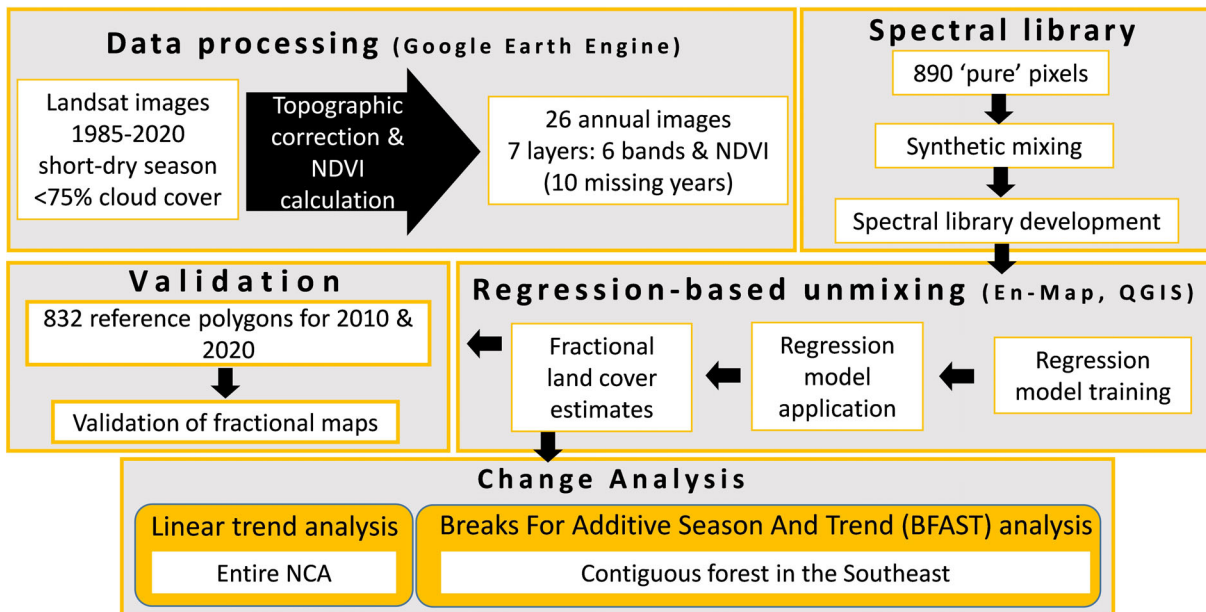

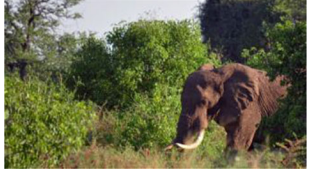









Figure 2. Methodological flowchart of our study.

Table 1. Description of the nine main land cover types of the NCA, according to Herlocker and Dirschl (1972) and Pratt et al. (1966).

| Land cover types | Description | Examples of land cover |
|------------------|--|---|
| Bareland | Minimal or no vegetation cover including bare rock, sand, saline or alkaline flats or riverine deposits. |  |
| Bushland | Closed shrub canopy comprising woody plants, bushes or trees, ranging from 3 to 6 m in height. |  |
| Cropland | Natural vegetation has been removed and replaced by other types of vegetation cover that require human activity to maintain it. |  |
| Forest | Closed canopy trees ranging between 7 and 40 m or more in height. The ground is mostly covered by bushes and shrubs making it difficult for animals to move through it. |  |
| Grassland | Grasses that vary between short (<25 cm) and tall (150 cm). In certain areas, herbs, scarred trees, or shrubs can occur. During the dry season and during droughts, it can be almost bareland. |  |
| Montane heath | Medium-sized vegetation (<1 m) including shrubs, grasses, ferns, and mosses, usually at higher altitudes. |  |
| Shrubland | Open canopy with medium-sized woody vegetation (<6 m in Pratt), surrounded by grass or bareland. Some trees and bushes can occur. |  |

(Continued)

Table 1. Continued.

| Land cover types | Description | Examples of land cover |
|------------------|--|---|
| Water | Ponds, lakes, rivers and swamps (with little or no vegetation cover). |  |
| Woodland | Open or continuous canopy with trees as tall as 20 m, often surrounded by shrubs, bushes or grass but not thicket. |  |

produced in an earlier study (Borges et al., 2020). This map was based on multi-temporal Sentinel-1 and 2 composites for 2019 with a 10 m spatial resolution. With higher quality input data used in its production and achieving high per-class and overall classification accuracies, we consider this dataset to be the best available and most suitable reference for informing our Landsat-based methodology in the present study.

Spectral library development

We employed a land cover classification schema based on the detailed surveys of the NCA undertaken in the 1960s by Herlocker and Dirschl (1972) and Pratt et al. (1966). This aligns with our previous work on land cover classification in the area (Borges et al., 2020), and is ecologically relevant both in terms of habitat usage by species and the management of the park. For instance, the highest densities of black rhino occur in bushland areas (Emslie, 2020), but in the NCA they can also be found in shrubland, open grasslands and closed-canopy forest, as such it becomes increasingly important to distinguish between these classes (Gadiye et al., 2016). In total, we assigned samples to nine land cover types, detailed in Table 1.

For the development of the spectral library, we collected 890 polygon samples from across the NCA, covering the nine land cover classes, based on our knowledge of the area, spectral information (Figs. S2 and S3), visualisation of high-resolution imagery within Google Earth Pro and the processed Landsat images (Fig. 2). The samples were distributed as follows: 20 for Bareland; 94 for Bushland; 11 for Cropland; 50 for Forest; 498 for Grassland; 19 for Montane heath; 82 for Shrubland; 13 for Water, and 103 for

Woodland. The sample size was proportional based on our earlier land cover map (Borges et al., 2020). Using a proportional sample size accommodates the greater spectral variability within the large classes (e.g. grassland) relative to the smaller more classes (e.g. montane heath). We compared multi-temporal Landsat images and aerial photography to select only pixels that remained unchanged throughout the study period (i.e. pseudo-invariant features). For each Landsat image, we extracted pixel values to produce an independent annual-level spectral library, creating a total of 26 libraries.

Synthetic mixing

To create fractional training data from our spectral library we used the EnMAP-box (version 3.6; EnMAP-Box Developers, 2019) software to generate synthetic mixture samples (Okujeni et al., 2013; Van der Linden et al., 2015). For each class, we generated 1000 synthetic samples, comprised of different fractional mixtures of all classes. The following processes, described in (Cooper et al., 2020), produced each synthetically mixed sample:

1. We established the likelihood for different multi-class combinations across each pixel and included endmembers according to this weighting. We set a 20% chance for a two classes mixture, 40% for a three classes mixture and 40% for a four classes mixture.
2. From the target class spectral library, one random endmember was pulled.
3. This selected endmember was randomly allocated a mixing fraction between 0 and 1.
4. Additional endmembers were randomly selected from the additional classes and added.

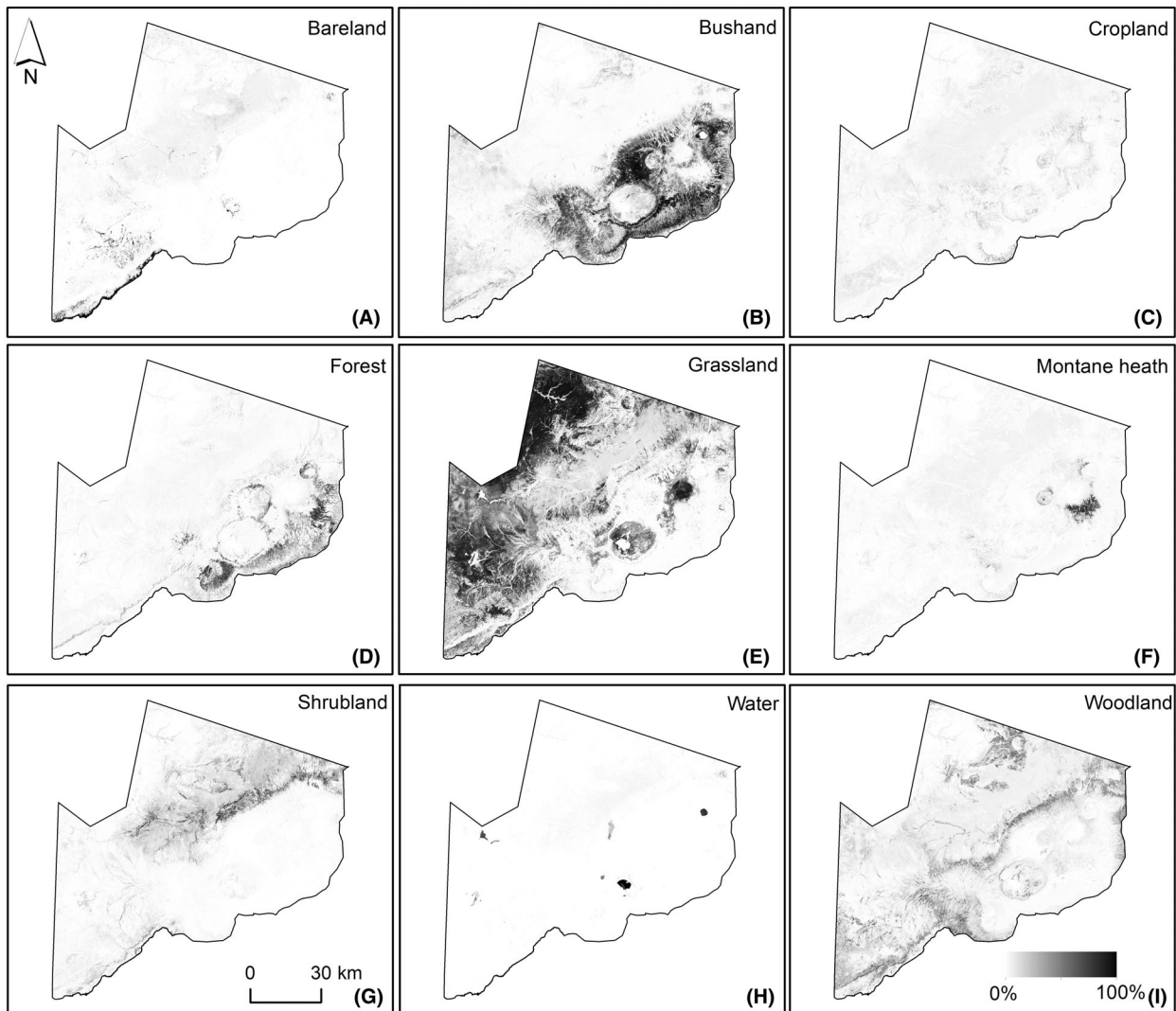


Figure 3. Fractional cover maps for the nine main land cover classes of the NCA in the year 2020. (A) Bareland, (B) Bushland, (C) Cropland, (D) Forest, (E) Grassland, (F) Montane heath, (G) Shrubland, (H) Water, (I) Woodland.

5. The newly added endmembers were randomly assigned mixing fraction, with the sum of all fractions equalling one.
6. Synthetically mixed spectra were generated based on linear combinations of the assigned mixing fractions. We repeated this process for every synthetic spectra. Finally, we added the original endmembers to the synthetic samples and assigned mixing fractions of one or zero for spectra belonging to target and non-target classes, respectively.

Regression-based unmixing

We used a Random Forest regression to map vegetation class fractions (Breiman, 2001). The Random Forest is a

non-parametric machine learning model based on ensembles of regression trees, popular for image classification and land cover mapping (Li et al., 2015; Rodriguez-Galiano et al., 2012; Symeonakis et al., 2018).

The regression-based unmixing was carried out in the EnMAP-Box 3.6 (EnMAP-Box Developers, 2019), an open-source QGIS plugin designed for advanced processing workflows of optical remote sensing data (Van der Linden et al., 2015). We repeated the unmixing procedure 10 times and averaged the predictions for each year, produced using the correspondent spectral library. This allowed the inclusion of multiple types of synthetic mixtures into the unmixing process while keeping the training sample size low (Okujeni et al., 2017).

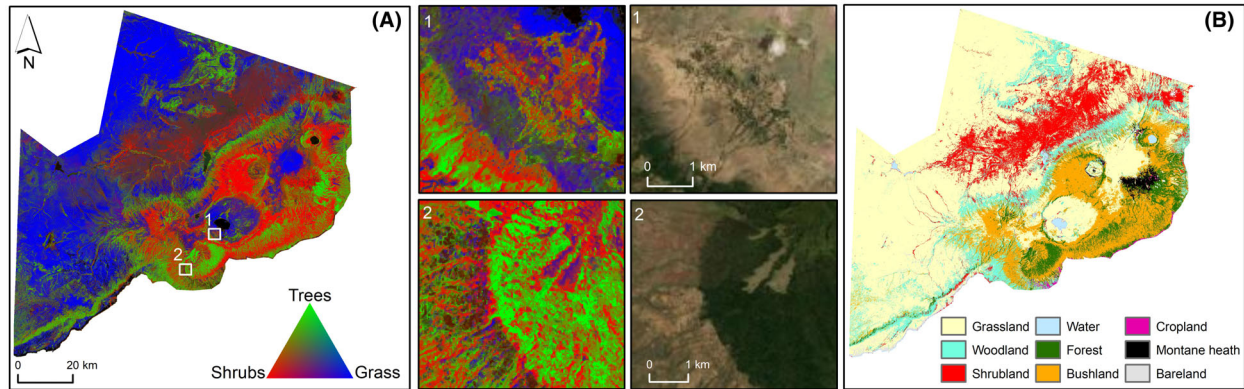


Figure 4. (A) RGB composite of the aggregated three main components of savannah landscapes: trees (G, forest and woodland), shrubs (R, bushland and shrubland) and grasses (B) for the year 2020; locations 1 and 2 are example subsets. (B) Land cover ('hard') classification for the year 2020.

Table 2. Accuracy of the fractional land covers for the NCA for the years 2010 and 2020.

| Land cover | | Bareland | Bushland | Cropland | Forest | Grassland | Montane heath | Shrubland | Water | Woodland |
|------------|-------|----------|----------|----------|--------|-----------|---------------|-----------|-------|----------|
| 2010 | MAE | 2.80 | 5.08 | 5.34 | 4.69 | 14.18 | 5.64 | 6.00 | 4.47 | 6.70 |
| | R^2 | 0.90 | 0.92 | 0.43 | 0.88 | 0.83 | 0.64 | 0.77 | 0.81 | 0.61 |
| | Bias | -3% | -6% | -8% | -6% | -1% | -8% | -3% | -6% | -8% |
| 2020 | MAE | 2.97 | 6.13 | 6.72 | 6.09 | 13.67 | 5.24 | 6.23 | 1.63 | 6.42 |
| | R^2 | 0.89 | 0.91 | 0.33 | 0.84 | 0.82 | 0.76 | 0.76 | 0.95 | 0.73 |
| | Bias | -2% | -10% | -9% | -7% | -1% | -8% | -2% | -10% | -8% |

Validation of fraction maps

A validation dataset centred on 2010 and 2020 was developed based on visual interpretation of high-resolution imagery in Google Earth Pro (Ludwig et al., 2016). Due to limited Google Earth imagery and uncertain dates for certain images, imagery between 2009 and 2014 was aggregated and compared to the 2010 fraction layers, and imagery between 2015 and 2020 was aggregated and compared to the 2020 layer. Validation of model predictions prior to 2010 was not possible as earlier images had substantially lower resolution or were unavailable. We validated the model predictions by using a stratified random sampling, based on best practise (Olofsson et al., 2014). We collected 416 reference pixels for each epoch, resulting in 832 reference pixels. For each reference pixel, a 10×10 grid of 3 m squares (Fig. S4) was used, and the class fractions were estimated by a researcher with local knowledge. For statistical validation, we calculated the bias, the coefficient of determination (R^2) and the mean absolute error (MAE) between the reference fractions and predicted fractions.

Change mapping

To detect changes in the fractional land cover, we employed two complementary time series analyses. Firstly, to detect the general land cover change, we performed a

linear regression against time on the annual fractional cover maps of each land cover class (Herrmann et al., 2005). Changes that were statistically ($p > 0.05$) or ecologically (cover in 2020 < 5%) insignificant were masked.

Secondly, to provide more detailed information on changes specifically in the upland forests, we applied the Break For Additive Season and Trend (BFAST) method (Verbesselt, Hyndman, Newnham, et al., 2010). BFAST is a piecewise linear regression approach that combines time-series decomposition with structural breakpoint detection. The statistical basis of BFAST is the decomposition of a time-series into trend, seasonal and residual components; with significant changes in the trend component detected by a moving sum of residuals (MOSUM) test. BFAST was originally developed for NDVI time-series, however, it is not specific for any type of data (Verbesselt, Hyndman, Newnham, et al., 2010) and has been applied to other vegetation indexes, rainfall data or Landsat bands. (Che et al., 2017; Higginbottom & Symeonakis, 2020; Horion et al., 2016; Morrison et al., 2018; Platt et al., 2018). We used the 'BFAST01' implementation of BFAST, which is tailored for non-seasonal (i.e. annual) data, and allowed for a single breakpoint to occur in the time series using a $P < 0.05$ significance threshold. The breakpoints identified by BFAST were then classified into six change types, based on de Jong et al. (2013): (1)

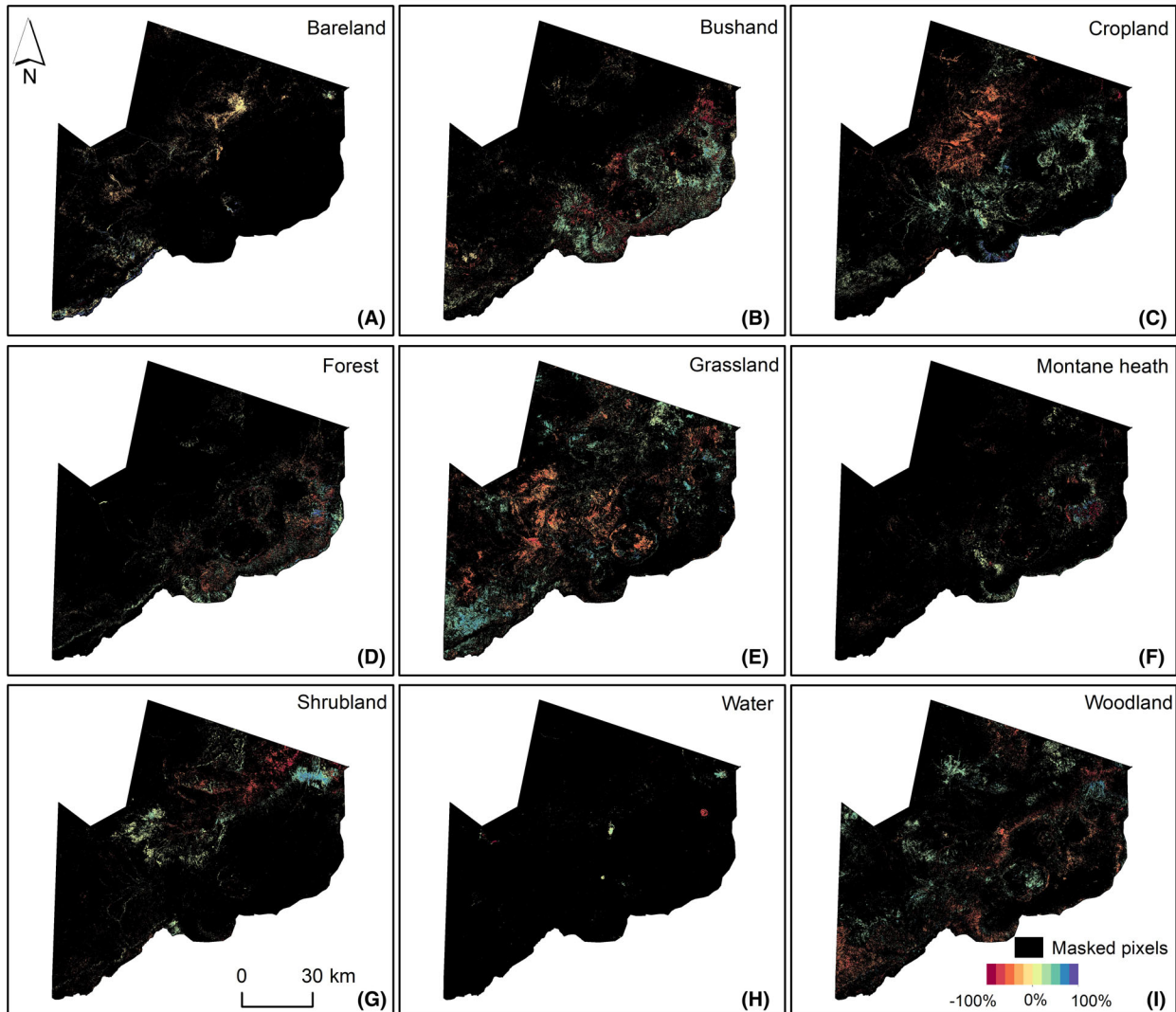


Figure 5. Land cover changed according to the linear trend analysis in the NCA between 1985 and 2020 for all land cover classes. (A) Bareland, (B) Bushland, (C) Cropland, (D) Forest, (E) Grassland, (F) Montane heath, (G) Shrubland, (H) Water, (I) Woodland.

monotonic: increase, (2) *monotonic: decrease*, (3) *reversal: increase to decrease*, (4) *reversal: decrease to increase*, (5) *interruption: increase with negative break*, and (6) *interruption decrease with positive break*.

Our logic for employing two time-series analyses is as follows: gradual changes (e.g. shrub encroachment, grassland degradation) will be best identified using monotonic trend analysis (Lewińska et al., 2020), whereas BFAST is well suited for identifying sudden changes and reversals that may be obscured within the long-term analysis. However, grasslands and non-woody areas will fluctuate more on an annual basis, due to climatic variation and benefit from a simpler change model. Furthermore, we employ trend analysis over direct comparison of the fractional cover maps to ensure our analysis is robust to

variation and noise in the input maps. We expect our annual fractional maps to contain errors and noise which may distort bi-temporal comparisons. This is analogous to post-classification cleaning of hard classification change detections, by removing illogical transitions (e.g. Griffiths et al., 2018) or applying statistical techniques such as Hidden Markov Models (e.g. Abercrombie & Friedl, 2016).

Results

Fraction maps

The predicted fractional land cover maps (Fig. 3) successfully distinguished the nine land cover types

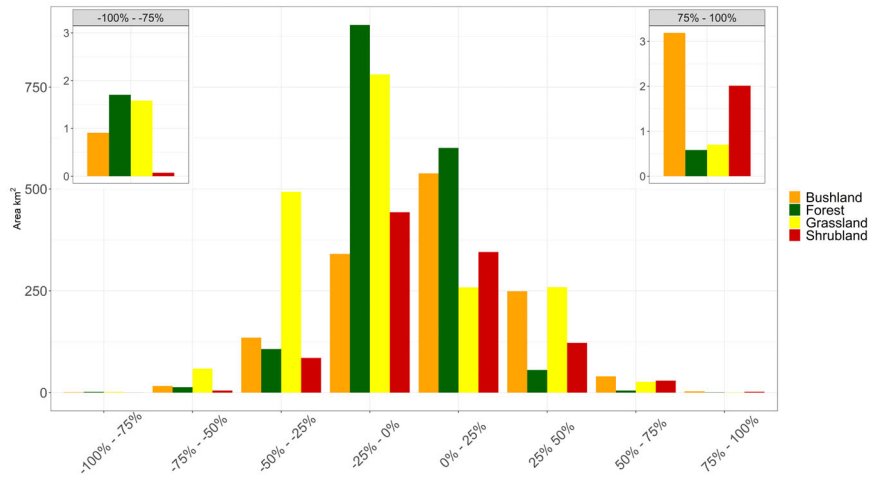


Figure 6. Statistically significant ($p < 0.05$) changes in land cover between 1985 and 2020 for forest, bushland, shrubland, and grassland.

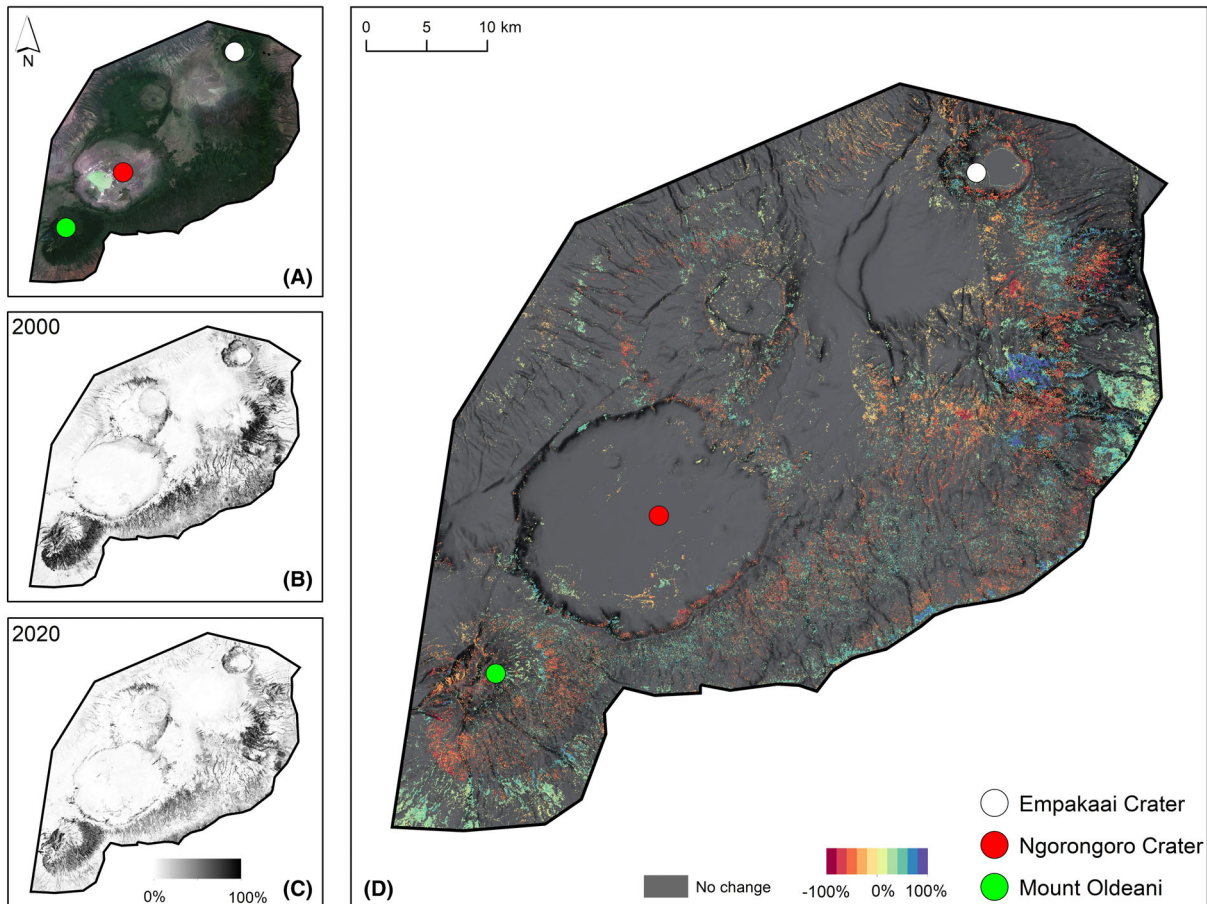


Figure 7. True colour composite Landsat image for the year 2000 (A). Fraction of forest cover in the NCA in the years 2000 (B) and 2020 (C). Forest cover change according to the linear trend analysis between 1985 and 2020 in the southeast of the NCA (D).

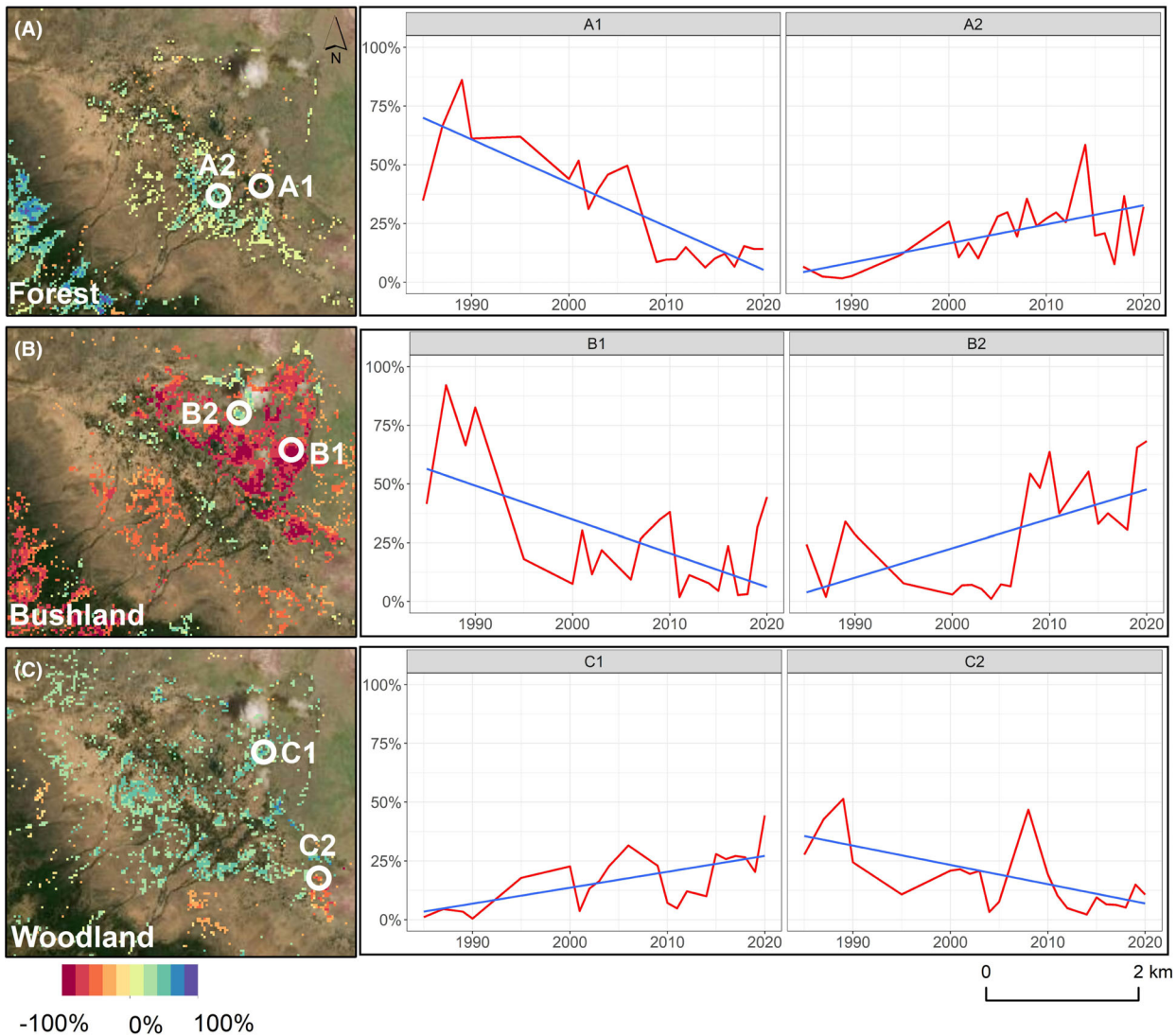


Figure 8. (A–C) and respective plots (A1 to C2): linear trend changes in forest, bushland, and woodland in the Lerai Forest (this area is the example Location 1 shown in Fig. 4).

(Table 1), and a discrete land cover map shown in Figure 4B was estimated from the fractional map of 2020 (Fig. 3). We were able to identify transitional areas with highly heterogeneous land cover (Fig. 3). For instance, most of the NCA is dominated by grassland (Fig. 3), which transitions into shrubland around the centre. The Highland area (Fig. 1A) is dominated by woody classes (bushland, woodland, forest). Figure 4A shows a red-green-blue composite of the land cover layers aggregated into three main components of savannah landscapes: trees (forest and woodland), shrubs (bushland and shrubland) and grasses (grassland). For bushland and forest, there are areas of clear separation (Fig. 4A) but there is also some degree of mixture (Fig. 3). The West

side of the NCA mostly comprises grassland (e.g. the Serengeti Plain) with some patchy shrubland around the Ang'ata Salei plain.

Validation statistics for the fractional land cover maps of 2010 and 2020 (MAE and R^2) are shown in Table 2 (full statistics in Tables S1 and S2 and scatterplots in Figs. S5 and S6). Most classes performed well, achieving accuracies between R^2 0.61 and 0.95 (Figs. S5 and S6). The lowest absolute errors occurred in the bareland class with an MAE of 2.8 for 2010 and water with an MAE of 1.63 for 2020. Cropland had the highest relative errors with R^2 of 0.43 and 0.33 for 2010 and 2020, respectively. Most cross-class confusion occurred in transition ecozones between grassland-bareland and grassland-

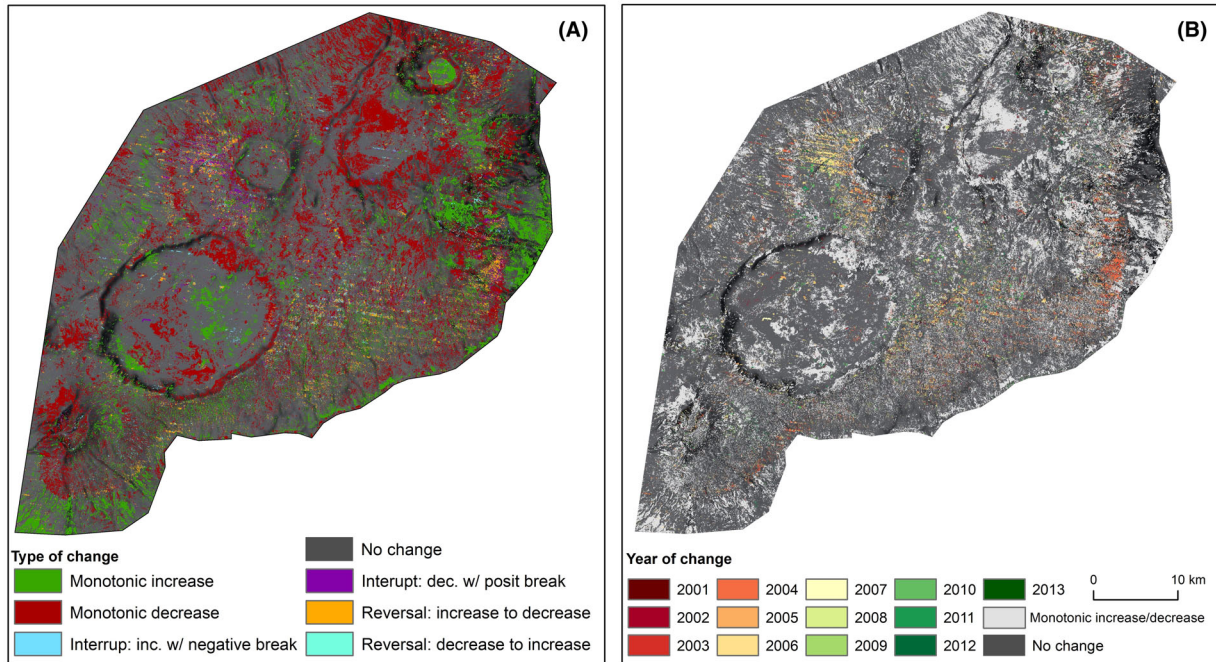


Figure 9. (A) BFAST trend analysis results for the southeast side of the NCA showing the type of change in forest cover; (B) the year of change in forest cover.

shrubland. This was expected due to the highly heterogeneous nature of these regions.

Linear trends

Linear trends for the NCA

Figure 5 shows the statistically significant ($p < 0.05$) linear trends for each individual and cover type. Areas with $<5\%$ cover in the respective class for 2020 were masked. There were notable increases and decreases for all land cover types with most of the change in the $\pm 25\%$ range (Fig. 6). The most common change in the NCA was decreasing forest by $\sim 25\%$ coverage, which affected roughly 900 km^2 (Figs. 5 and 6). The second most common change was grassland coverage declining by 25% , which affected roughly 782 km^2 (Figs. 5 and 6). A sizeable amount of grassland also experienced a decline of up to 50% ($\sim 493 \text{ km}^2$), mostly in the Serengeti plains (Figs. 5 and 6).

A majority of forest cover is located in the eastern part of the NCA. Figures 7B and C show a clear reduction in fractional cover, particularly visible around Mount Oldeni, throughout the highlands and on the south-east side of the Crater rim (Fig. 7D). There is also some patchy increase in forest cover, ranging between 25% and 75% cover in the highlands, outside the NCA border near Mount Oldeani and in the montane areas (Fig. 7D).

Linear trends: the case of Lerai Forest

Contrarily to its name, the Lerai Forest mostly comprises low woodland and bushland with some forest and shrubland. According to our findings, there were both increases and decreases in the fractional cover of forest, bushland and woodland (Figs. 8A and C). The most obvious change in the Lerai Forest was the decrease in bushland cover, ranging between -25% and -75% (covering 1.6 km^2), and the increase in woodland ($+25\%$ covering 1 km^2 ; Figs. 8B and C). However, the expansion of woody vegetation, specifically forest and woodland occurred mostly in the southwest side of the Lerai Forest (Fig. 8A and C; Figure S7).

BFAST trends

BFAST trends in the NCA

Most of the forest change detected by BFAST consisted of monotonic increases and decreases (Fig. 9A). Forest loss was widespread with some focal points in the rim of the Crater, around Mount Oldeani and Empakai Crater. Throughout the highlands, there was also a reversal where forest cover increased but then started to decrease. These shifts in the vegetation occurred mostly between 2004 and 2009 (Fig. 9B).

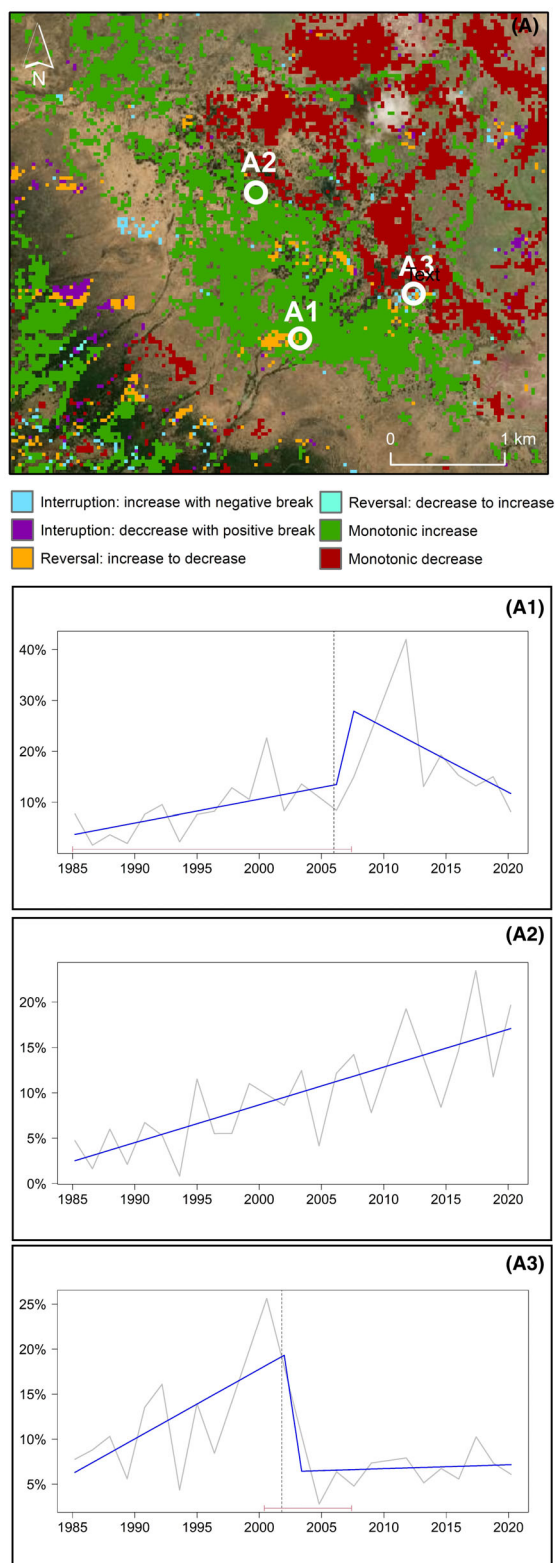


Figure 10. Outcome of the trend analysis using BFAST for the Lerai Forest (A). Locations A1–A3 are used as examples of time-series plots at the individual pixel level.

BFAST trends: the case of Lerai Forest

The change map produced using BFAST for the Lerai Forest is shown in Figure 10. In the northeast side of the Lerai Forest, BFAST detected a consistent monotonic decrease in forest cover (Fig. 10). Additionally, a large cluster that experienced a monotonic increase occurred on the southwest side of the Forest (Fig. 10). Although significant, some of those changes were subtle (<25%; Fig. 10, location A2) when compared to others (Fig. 10, location A1). For instance, in location A2 (Fig. 10) there was a consistent increase in cover which remained low. In A1, forest cover increased until 2008, when it started to decrease but the changes were more pronounced than in A2.

Discussion

Understanding land cover dynamics is increasingly important to improve habitat monitoring, preserve biodiversity and ensure sustainable development (Reed et al., 2009). Over the last 30 years, the NCA has undergone considerable changes but these remain poorly understood due to lack of robust information and detailed maps. Here, we demonstrate a Landsat-based monitoring strategy, combining synthetic unmixing, machine learning regression and time-series analysis, to quantify sub-pixel change in nine land cover classes. Our fractional cover maps for 2010 and 2020 achieved high accuracies for most land cover types (Table 2, Tables S1 and S2 and Figs. S5 and S6), distinguishing the nine main land cover classes but also identifying transitional areas with heterogeneous vegetation (Figs. 3 and 4A). Out of our nine land cover types, only cropland scored low accuracies (R^2 0.43 and 0.33 for 2010 and 2020, respectively), while the other classes high accuracies ($R^2 > 0.6$, Table 2). Souverijns et al. (2020) and Senf et al. (2020) achieved similar accuracies for comparable land cover types, but Nabil et al. (2020) reported low accuracies for cropland in the Sahel regions. Using fractional cover maps has proven advantageous, as it allows for the detection of more subtle land cover variability and changes that cannot be captured by discrete classifications (Senf et al., 2020; Souverijns et al., 2020; Suess et al., 2018).

Between 1985 and 2020, we identified significant land cover changes; in particular, declines in forest and grassland cover (Figs. 5–7). The most common change using the linear trend analysis was a decrease in forest coverage by ~25%, which affected roughly 900 km² (Fig. 6). BFAST also detected a similar trend in the highlands, with a monotonic decrease in forest throughout the period (Fig. 9A). Contrarily, there was an increase in bushland cover by 25%, covering 440 km² (Fig. 6). These changes are consistent with field studies

that have identified forest conversion into bushland due to the removal of larger trees (Amiyo, 2006; Masao et al., 2015; TAWIRI & NCAA, 2020). A report by the Tanzania Wildlife Research Institute (TAWIRI) and the Ngorongoro Conservation Area Authority (NCAA) in 2020 also found a decrease in forest cover between 1978 and 2018. These changes were linked to human disturbances namely clearing for settlement or cultivation and searching for thatching materials and fuel wood (Kija et al., 2020; Masao et al., 2015; TAWIRI & NCAA, 2020). In addition (Mills, 2006), studied the dieback of *Acacia xanthophloea* (commonly known as fever tree which can reach 25 metres) in Ngorongoro Crater identified natural disturbances, specifically herbivory (mainly by elephants, *Loxodonta africana*), disease and salinity as contributors for the demise of large trees.

Forest degradation has been reported across Africa and is a common indicator of land degradation (Ahrends et al., 2021; Bukombe et al., 2018; McNicol et al., 2018). In addition, forests promote carbon sequestration and therefore, directly affect global carbon budgets and climate change (McNicol et al., 2018; Venter et al., 2018). In the NCA, degradation of forests threatens the availability of good habitat for wildlife species adapted to such particular forest type. Souverijns et al. (2020) mapped 30 years of land cover changes over the Sudano-Sahel and detected forest degradation based on fractional land cover maps. Meanwhile, McNicol et al. (2018), used radar data to study losses in carbon in savannahs, identifying deforestation and degradation proximate to roads and urban areas but gains in remote regions. Our results support those findings and show that Landsat data and fractional cover maps can be used to detect and monitor forest degradation. The use of Landsat to map forest degradation processes is highly beneficial, due to the temporal length of the Landsat archive relative to radar data.

Serengeti plains

The loss of palatable grasses has been identified as a threat to wildlife, the Maasai pastoralists and the NCA ecosystem as a whole (Amiyo, 2006; Mills et al., 2006). We found that grassland cover decreased in the NCA during the study period (Figs. 5 and 6). Figure 6 shows between 25% and 50% decrease in grassland cover (493 km² to 782 km²), mostly located in the Serengeti plains (Figs. 5 and 6). In the same area, the increase in shrubland (~345 km²) and woodland cover (~497 km²) is also visible (Figs. 5 and 6). Previous research reported a decline in grassland and woody encroachment in the NCA which supports our findings

(Amiyo, 2006; Masao et al., 2015; Niboye, 2010). The no-burning policy imposed in the 1980s was identified as the main driver for land cover changes, specifically woody encroachment in the NCA (Amiyo, 2006; Home-wood et al., 2001). In addition, grazing pressure, by wildlife and livestock, also facilitates the development of woody plant communities by removing fine fuels and reducing fire frequency and intensity (Archer et al., 2017; Smit et al., 2010).

Shrub encroachment, often linked to grassland decline and land degradation, is a serious threat to ecosystem services and biodiversity (Higginbottom & Symeonakis, 2020; Symeonakis et al., 2018). Previous research found an increasing trend of woody cover throughout Africa (Higginbottom et al., 2018; Ludwig et al., 2019; Symeonakis et al., 2018). Venter et al. (2018) reported that encroachment is accelerating over time and that African savannahs are at high risk of widespread vegetation change. Stevens et al. (2016) measured woody cover change between 1940 and 2010 and found similar results in areas with low rainfall (<650 mm). Contrarily to forest degradation, shrub encroachment can have a positive impact on aboveground carbon storage (McNicol et al., 2018). However, the loss of grassland areas raises issues for wildlife, the Maasai pastoralists and their livestock (Niboye, 2010). In the Serengeti plains, densification and encroachment of woody cover can have a negative effect on groundwater recharge, grazing potential (Angassa & Baars, 2000; Stevens et al., 2017), tourism (Gray & Bond, 2013), and is related to increase costs for woody vegetation clearing (Grossman & Gandar, 1989). Woody encroachment into grasslands can potentially be reversed by a combination of management (frequent fires) and climatic events (drought; Roques et al., 2001). In these areas using fire as a management strategy can decrease shrub and invasive species, and has been successfully employed throughout the continent (Sankaran et al., 2005; Venter et al., 2018). Additionally, reducing grazing pressure by decreasing livestock numbers can positively affect grassland areas (Archer et al., 2017). As such, given the infeasibility of reducing livestock numbers, trailing fire management to assess the potential for limiting encroachment and improving rangeland condition may be beneficial.

Lerai Forest

The earliest records of change in the NCA date back to the 1960s when the dieback of the Lerai forest was first suggested (Amiyo, 2006; Mills, 2006). Our results show contrasting trends: a significant decline in woody cover within the original range of Lerai Forest (Fig. S7) and an overall increase in forest cover in the periphery (Figs. 8A and 10).

These results suggest that Lerai Forest is re-establishing outside its original range (Amiyo, 2006). Historically, mature fever trees *Acacia xanthophloea*, which can reach heights up to 25 meters and require high water tables (Homewood et al., 2001), dominated the Lerai Forest, however since their decline they have not been replaced by young *Acacia xanthophloea* trees (Amiyo, 2006). The decrease in groundwater availability, due to a higher influx of tourism and diversion of streams, as well as floods of the salt lake, Lake Magadi, contributed to an increase in soil salinity, which negatively affects vegetation (Amiyo, 2006; Boone et al., 2007; Mills, 2006). Mills (2006) suggested that sodicity (e.g. the accumulation of sodium salt in the soil) can exacerbate salinity-induced drought stress in vegetation, by limiting entry of rainwater into the soil, which was already low due to a reduced rainfall (Fig. S1). Furthermore, sodicity can promote sodium concentrations in trees, which has an additional detrimental effect by attracting elephants and other herbivores (Homewood et al., 2001; Mills, 2006). Management strategies were implemented and in 2006, the stream was diverted back to supplying the Forest (Mills, 2006, Fig. 10, location A1). This increased the freshwater supply to the area and promoted the flushing of salts from the soil (Mills, 2006). The southwest side, closer to the Crater rim, is more fertile and has a lower soil salinity due to its proximity to the stream, which explains the increase in forest and woodland cover (Fig. 8A and C; 10 location A1; Elisante et al., 2013, Mills, 2006). Exclusion of elephants from Lerai was considered in 2006 but was never implemented (Mills, 2006). The dieback in Lerai may be jeopardising the long-term conservation of the black rhinoceros *Diceros bicornis michaeli* population in the caldera (Mills, 2006). Historically, the Lerai Forest was used for shelter and browse by the rhinos and it has been suggested it was also critical for hiding newborn rhinos from predators (Goddard, 1967, 1968). Consequently, the recovery of the Lerai Forest is an essential priority for the success of black rhino population in the NCA (Mills et al., 2006).

Conclusion

Mapping and quantifying land cover change is important to support habitat monitoring, preserve biodiversity and ensure sustainable development (Reed et al., 2009). Savannah landscapes, such as the NCA, however, are complex heterogeneous combinations of vegetation. Here we demonstrate that a regression-based unmixing with synthetic training data-based approach is effective in the fractional mapping of spectrally similar land cover types. In addition, the combination of linear trend and BFAST time-series analysis provided highly detailed and complementary insights into land cover change dynamics throughout the 35-year study period. We identified two

dominant land change dynamics: the degradation of uplands forest into bushland, and a transition from grassland to shrubland in the Serengeti Plains. These changes threaten the wellbeing of livestock, and consequently the livelihoods of pastoralists but also grazing dependent wildlife. These changes are likely due to a combination of climate change, shifting rainfall patterns, herbivory; and human activities, namely, management policies, tourism and increasing human populations and livestock. In conclusion, we provide much needed and highly accurate information on long-term land cover changes in the NCA, which can support sustainable management and conservation. In addition, our methodological approach can be applied elsewhere to understand savannah landscape changes.

Conflict of Interest

The authors declare no conflict of interest.

Acknowledgement

Open access funding enabled and organized by Projekt DEAL.

References

- Abercrombie, S.P. & Friedl, M.A. (2016) Improving the consistency of multitemporal land cover maps using a hidden Markov model. *IEEE Transactions on Geoscience and Remote Sensing*, **54**(2), 703–713. <https://doi.org/10.1109/TGRS.2015.2463689>
- Adole, T., Dash, J. & Atkinson, P.M. (2016) A systematic review of vegetation phenology in Africa. *Ecological Informatics*, **34**, 117–128. <https://doi.org/10.1016/j.ecoinf.2016.05.004>
- Ahrends, A., Bulling, M.T., Platts, P.J., Swetnam, R., Ryan, C., Doggart, N. et al. (2021) Detecting and predicting forest degradation: a comparison of ground surveys and remote sensing in Tanzanian forests. *Plants, People Planet*, **3**(3), 268–281. <https://doi.org/10.1002/ppp3.10189>
- Amiyo, T. A. (2006). *Ngorongoro crater rangelands: condition, management and monitoring: Vol.* MSc thesis. University of Kwazulu-Natal, South Africa.
- Angassa, A. & Baars, R.M.T. (2000) Ecological condition of encroached and non-encroached rangelands in Borana, Ethiopia. *African Journal of Ecology*, **38**(4), 321–328. <https://doi.org/10.1046/j.1365-2028.2000.00250>
- Archer, S.R., Andersen, E.M., Predick, K.I., Schwinning, S., Steidl, R.J. & Woods, S.R. (2017) Woody plant encroachment: causes and consequences. In: Briske, D.D. (Ed.) *Rangeland systems: processes, management and challenges*. Springer International Publishing, pp. 25–84. https://doi.org/10.1007/978-3-319-46709-2_2

- Baumann, M., Levers, C., Macchi, L., Bluhm, H., Waske, B., Gasparri, N.I. et al. (2018) Mapping continuous fields of tree and shrub cover across the Gran Chaco using Landsat 8 and Sentinel-1 data. *Remote Sensing of Environment*, **216**, 201–211. <https://doi.org/10.1016/j.rse.2018.06.044>
- Boone, R.B., Galvin, K.A., Thornton, P.K., Swift, D.M. & Coughenour, M.B. (2006) Cultivation and conservation in Ngorongoro conservation area, Tanzania. *Human Ecology*, **34**(6), 809–828. <https://doi.org/10.1007/s10745-006-9031-3>
- Boone, R.B., Lackett, J.M., Galvin, K.A., Ojima, D.S. & Tucker, C.J. (2007) Links and broken chains: evidence of human-caused changes in land cover in remotely sensed images. *Environmental Science & Policy*, **10**(2), 135–149. <https://doi.org/10.1016/j.envsci.2006.09.006>
- Borges, J., Higginbottom, T.P., Symeonakis, E. & Jones, M. (2020) Sentinel-1 and Sentinel-2 data for Savannah land cover mapping: optimising the combination of sensors and seasons. *Remote Sensing*, **12**(23), 3862. <https://doi.org/10.3390/rs12233862>
- Breiman, L. (2001) Random forests. *Machine Learning*, **45**(1), 5–32. <https://doi.org/10.1023/A:1010933404324>
- Bukombe, J., Smith, S., Kija, H., Loishooki, A., Sumay, G., Mwita, M. et al. (2018) Fire regulates the abundance of alien plant species around roads and settlements in the Serengeti National Park. *Management of Biological Invasions*, **9**(3), 357–367. <https://doi.org/10.3391/mbi.2018.9.3.17>
- Che, X., Yang, Y., Feng, M., Xiao, T., Huang, S., Xiang, Y. et al. (2017) Mapping extent dynamics of Small Lakes using downscaling MODIS surface reflectance. *Remote Sensing*, **9**(1), 82. <https://doi.org/10.3390/rs9010082>
- Cooper, S., Okujeni, A., Jänicke, C., Clark, M., van der Linden, S. & Hostert, P. (2020) Disentangling fractional vegetation cover: regression-based unmixing of simulated spaceborne imaging spectroscopy data. *Remote Sensing of Environment*, **246**, 111856. <https://doi.org/10.1016/j.rse.2020.111856>
- de Jong, R., Verbesselt, J., Zeileis, A. & Schaepman, M.E. (2013) Shifts in global vegetation activity trends. *Remote Sensing*, **5**(3), 1117–1133. <https://doi.org/10.3390/rs5031117>
- Elisante, F., Tarimo, M.T. & Ndakidemi, P.A. (2013) Distribution and abundance of *Datura stramonium* in Ngorongoro conservation area. *American Journal of Research Communication*, **1**(12), 182–196.
- Emslie, R. (2020). *Diceros bicornis*. *The IUCN Red List of Threatened Species 2020: E.T6557A152728945*. <https://doi.org/10.2305/IUCN.UK.2020-1.RLTS.T6557A152728945.en>.
- EnMAP-Box Developers. (2019). *EnMAP-Box 3—A QGIS Plugin to process and visualize hyperspectral remote sensing data*.
- Estes, R.D., Atwood, J.L. & Estes, A.B. (2006) Downward trends in Ngorongoro crater ungulate populations 1986–2005: conservation concerns and the need for ecological research. *Biological Conservation*, **131**(1), 106–120. <https://doi.org/10.1016/j.biocon.2006.02.009>
- Gadiye, D.E. & Koskei, A. (2016) Spatial-temporal distribution of the black rhino population in the Ngorongoro crater, Tanzania. *International Journal of Biological Research*, **4**(2), 232–236.
- Goddard, J. (1967) Home range, behaviour and recruitment rates of two black rhinoceros populations. *African Journal of Ecology*, **5**(1), 133–150. <https://doi.org/10.1111/j.1365-2028.1967.tb00768.x>
- Goddard, J. (1968) Food preferences of two black rhinoceros populations. *East African Wildlife Journal*, **6**, 1–18.
- Gorelick, N., Hancher, M., Dixon, M., Ilyushchenko, S., Thau, D. & Moore, R. (2017) Google earth engine: planetary-scale geospatial analysis for everyone. *Remote Sensing of Environment*, **202**, 18–27. <https://doi.org/10.1016/j.rse.2017.06.031>
- Gray, E.F. & Bond, W.J. (2013) Will woody plant encroachment impact the visitor experience and economy of conservation areas? *Koedoe*, **55**(1). <https://doi.org/10.4102/koedoe.v55i1.1106>
- Griffiths, P., Jakimow, B. & Hostert, P. (2018) Reconstructing long term annual deforestation dynamics in Pará and Mato Grosso using the Landsat archive. *Remote Sensing of Environment*, **216**, 497–513. <https://doi.org/10.1016/j.rse.2018.07.010>
- Grogan, K., Pflugmacher, D., Hostert, P., Verbesselt, J. & Fensholt, R. (2016) Mapping clearances in tropical dry forests using breakpoints, trend, and seasonal components from MODIS time series: does Forest type matter? *Remote Sensing*, **8**(8), 657. <https://doi.org/10.3390/rs8080657>
- Grossman, D. & Gandar, M.V. (1989) Land transformation in south African savanna regions. *South African Geographical Journal*, **71**(1), 38–45. <https://doi.org/10.1080/03736245.1989.9713503>
- Gu, D. & Gillespie, A. (1998) Topographic normalization of Landsat TM images of Forest based on subpixel sun–canopy–sensor geometry. *Remote Sensing of Environment*, **64**(2), 166–175. [https://doi.org/10.1016/S0034-4257\(97\)00177-6](https://doi.org/10.1016/S0034-4257(97)00177-6)
- Harris, W., de Kort, S., Bettridge, C., Borges, J., Cain, B., Hamadi Dulle, I. et al. (2020) Short communication: a learning network approach to resolve conservation challenges in the Ngorongoro conservation area. *African Journal of Ecology*, **1**–6. <https://doi.org/10.1111/aje.12815>
- Herlocker, D.J. & Dirschl, H.J. (1972) *Vegetation of the Ngorongoro conservation area, Tanzania*. Ottawa: Environment Canada.
- Herrmann, S.M., Anyamba, A. & Tucker, C.J. (2005) Recent trends in vegetation dynamics in the African Sahel and their relationship to climate. *Global Environmental Change*, **15**(4), 394–404. <https://doi.org/10.1016/j.gloenvcha.2005.08.004>
- Higginbottom, T.P. & Symeonakis, E. (2014) Assessing land degradation and desertification using vegetation index data: current frameworks and future directions. *Remote Sensing*, **6**(10), 9552–9575. <https://doi.org/10.3390/rs6109552>

- Higginbottom, T.P. & Symeonakis, E. (2020) Identifying ecosystem function shifts in Africa using breakpoint analysis of long-term NDVI and RUE data. *Remote Sensing*, **12**(11), 1894. <https://doi.org/10.3390/rs12111894>
- Higginbottom, T.P., Symeonakis, E., Meyer, H. & van der Linden, S. (2018) Mapping fractional woody cover in semi-arid savannahs using multi-seasonal composites from Landsat data. *ISPRS Journal of Photogrammetry and Remote Sensing*, **139**, 88–102. <https://doi.org/10.1016/j.isprsjprs.2018.02.010>
- Homewood, K., Lambin, E.F., Coast, E., Kariuki, A., Kikula, I., Kivelia, J. et al. (2001) Long-term changes in Serengeti-Mara wildebeest and land cover: pastoralism, population, or policies? *Proceedings of the National Academy of Sciences of the United States of America*, **98**(22), 12544–12549. <https://doi.org/10.1073/pnas.221053998>
- Horion, S., Prishchepov, A.V., Verbesselt, J., de Beurs, K., Tagesson, T. & Fensholt, R. (2016) Revealing turning points in ecosystem functioning over the northern Eurasian agricultural frontier. *Global Change Biology*, **22**(8), 2801–2817. <https://doi.org/10.1111/gcb.13267>
- Kija, H.K., Ogotu, J.O., Mangewa, L.J., Bukombe, J., Verones, F., Graae, B.J. et al. (2020) Land use and land cover change within and around the greater Serengeti ecosystem, Tanzania. *American Journal of Remote Sensing*, **8**(1), 1–19. <https://doi.org/10.11648/j.ajrs.20200801.11>
- Lewińska, K.E., Hostert, P., Buchner, J., Bleyhl, B. & Radeloff, V.C. (2020) Short-term vegetation loss versus decadal degradation of grasslands in the Caucasus based on cumulative endmember fractions. *Remote Sensing of Environment*, **248**, 111969. <https://doi.org/10.1016/j.rse.2020.111969>
- Li, X.J., Cheng, X.W., Chen, W.T., Chen, G. & Liu, S.W. (2015) Identification of forested landslides using LiDAR data, object-based image analysis, and machine learning algorithms. *Remote Sensing*, **7**(8), 9705–9726. <https://doi.org/10.3390/rs70809705>
- Liu, Y.Y., van Dijk, A., de Jeu, R.A.M., Canadell, J.G., McCabe, M.F., Evans, J.P. et al. (2015) Recent reversal in loss of global terrestrial biomass. *Nature Climate Change*, **5**(5), 470–474. <https://doi.org/10.1038/nclimate2581>
- Ludwig, A., Meyer, H. & Naus, T. (2016) Automatic classification of Google earth images for a larger scale monitoring of bush encroachment in South Africa. *International Journal of Applied Earth Observation and Geoinformation*, **50**, 89–94. <https://doi.org/10.1016/j.jag.2016.03.003>
- Ludwig, M., Morgenthal, T., Detsch, F., Higginbottom, T.P., Lezama Valdes, M., Nauß, T. et al. (2019) Machine learning and multi-sensor based modelling of woody vegetation in the Molopo area, South Africa. *Remote Sensing of Environment*, **222**, 195–203. <https://doi.org/10.1016/j.rse.2018.12.019>
- Lyimo, E., Kohi, E., Maliti, H., Kimaro, J., Mwita, M., & Kija, H. (2020). *Population trends in the Ngorongoro Conservation Area since 1995 to 2018*. <https://doi.org/10.13140/RG.2.2.14384.38401>.
- Makacha, S., Molle, C.L. & Rwezaura, J. (1979) Conservation status of the black rhinoceros (*Diceros bicornis* L) in the Ngorongoro crater, Tanzania. *African Journal of Ecology*, **17**(2), 97–103. <https://doi.org/10.1111/j.1365-2028.1979.tb00461>
- Manzano, P., & Yamat, L. (2018). *Livestock sector in the Ngorongoro District: analysis, shortcomings and options for improvement*. <https://doi.org/10.13140/RG.2.2.33893.86240>.
- Masao, C.A., Makoba, R. & Sosovele, H. (2015) Will Ngorongoro conservation area remain a world heritage site amidst increasing human footprint? *International Journal of Biodiversity and Conservation*, **7**(9), 394–407. <https://doi.org/10.5897/IJBC2015.0837>
- Masek, J.G., Vermote, E.F., Saleous, N.E., Wolfe, R., Hall, F.G., Huemmrich, K.F. et al. (2006) A Landsat surface reflectance dataset for North America, 1990–2000. *IEEE Geoscience and Remote Sensing Letters*, **3**(1), 68–72. <https://doi.org/10.1109/lgrs.2005.857030>
- Mathieu, R., Naidoo, L., Cho, M.A., Leblon, B., Main, R., Wessels, K. et al. (2013) Toward structural assessment of semi-arid African savannahs and woodlands: the potential of multitemporal polarimetric RADARSAT-2 fine beam images. *Remote Sensing of Environment*, **138**, 215–231. <https://doi.org/10.1016/j.rse.2013.07.011>
- McNicol, I.M., Ryan, C.M. & Mitchard, E.T.A. (2018) Carbon losses from deforestation and widespread degradation offset by extensive growth in African woodlands. *Nature Communications*, **9**(1), 3045. <https://doi.org/10.1038/s41467-018-05386-z>
- Mills, A., Morkel, P., Amiyo, A., Runyoro, V., Borner, M. & Thirgood, S. (2006) Managing small populations in practice: black rhino *Diceros bicornis michaeli* in the Ngorongoro crater, Tanzania. *Oryx*, **40**(3), 319–323. <https://doi.org/10.1017/s0030605306000901>
- Mills, A.J. (2006) The role of salinity and sodicity in the dieback of *Acacia xanthophloea* in Ngorongoro caldera, Tanzania. *African Journal of Ecology*, **44**(1), 61–71. <https://doi.org/10.1111/j.1365-2028.2006.00616.x>
- Moore, R. T., & Hansen, M. C. (2011). *Google earth engine: a new cloud-computing platform for global-scale earth observation data and analysis*. AGU Fall Meeting Abstracts, 2011, IN43C-02
- Morrison, J., Higginbottom, T.P., Symeonakis, E., Jones, M.J., Omengo, F., Walker, S.L. et al. (2018) Detecting vegetation change in response to confining elephants in forests using MODIS time-series and BFAST. *Remote Sensing*, **10**(7). <https://doi.org/10.3390/rs10071075>
- Nabil, M., Zhang, M., Bofana, J., Wu, B., Stein, A., Dong, T. et al. (2020) Assessing factors impacting the spatial discrepancy of remote sensing based cropland products: a case study in Africa. *International Journal of Applied Earth Observation and Geoinformation*, **85**, 102010. <https://doi.org/10.1016/j.jag.2019.102010>

- Niboye, E.P. (2010) Vegetation cover changes in Ngorongoro conservation area from 1975 to 2000: the importance of remote sensing images. *The Open Geography Journal*, **3**(1), 15–27.
- Okujeni, A., van der Linden, S., Suess, S. & Hostert, P. (2017) Ensemble learning from synthetically mixed training data for quantifying urban land cover with support vector regression. *IEEE Journal of Selected Topics in Applied Earth Observations and Remote Sensing*, **10**(4), 1640–1650. <https://doi.org/10.1109/JSTARS.2016.2634859>
- Okujeni, A., van der Linden, S., Tits, L., Somers, B. & Hostert, P. (2013) Support vector regression and synthetically mixed training data for quantifying urban land cover. *Remote Sensing of Environment*, **137**, 184–197. <https://doi.org/10.1016/j.rse.2013.06.007>
- Olofsson, P., Foody, G.M., Herold, M., Stehman, S.V., Woodcock, C.E. & Wulder, M.A. (2014) Good practices for estimating area and assessing accuracy of land change. *Remote Sensing of Environment*, **148**, 42–57. <https://doi.org/10.1016/j.rse.2014.02.015>
- Pellikka, P.K.E., Heikinheimo, V., Hietanen, J., Schäfer, E., Siljander, M. & Heiskanen, J. (2018) Impact of land cover change on aboveground carbon stocks in Afromontane landscape in Kenya. *Applied Geography*, **94**, 178–189. <https://doi.org/10.1016/j.apgeog.2018.03.017>
- Platt, R.V., Manthos, D. & Amos, J. (2018) Estimating the creation and removal date of fracking ponds using trend analysis of Landsat imagery. *Environmental Management*, **61**(2), 310–320. <https://doi.org/10.1007/s00267-017-0983-4>
- Poulter, B., Frank, D., Ciais, P., Myneni, R.B., Andela, N., Bi, J. et al. (2014) Contribution of semi-arid ecosystems to interannual variability of the global carbon cycle. *Nature*, **509**(7502), 600. <https://doi.org/10.1038/nature13376>
- Pratt, D.J., Greenway, P.J. & Gwynne, M.D. (1966) A classification of east African rangeland, with an appendix on terminology. *The Journal of Applied Ecology*, **3**(2), 369. <https://doi.org/10.2307/2401259>
- Prince, S.D. & Tucker, C.J. (1986) Satellite remote sensing of rangelands in Botswana II. NOAA AVHRR and herbaceous vegetation. *International Journal of Remote Sensing*, **7**(11), 1555–1570. <https://doi.org/10.1080/01431168608948953>
- Reed, D.N., Anderson, T.M., Dempewolf, J., Metzger, K. & Serneels, S. (2009) The spatial distribution of vegetation types in the Serengeti ecosystem: the influence of rainfall and topographic relief on vegetation patch characteristics. *Journal of Biogeography*, **36**(4), 770–782. <https://doi.org/10.1111/j.1365-2699.2008.02017.x>
- Rodriguez-Galiano, V.F., Ghimire, B., Rogan, J., Chica-Olmo, M. & Rigol-Sanchez, J.P. (2012) An assessment of the effectiveness of a random forest classifier for land-cover classification. *ISPRS Journal of Photogrammetry and Remote Sensing*, **67**, 93–104. <https://doi.org/10.1016/j.isprsjprs.2011.11.002>
- Roques, K.G., O'Connor, T.G. & Watkinson, A.R. (2001) Dynamics of shrub encroachment in an African savanna: relative influences of fire, herbivory, rainfall and density dependence. *Journal of Applied Ecology*, **38**(2), 268–280. <https://doi.org/10.1046/j.1365-2664.2001.00567.x>
- Sankaran, M., Hanan, N.P., Scholes, R.J., Ratnam, J., Augustine, D.J., Cade, B.S. et al. (2005) Determinants of woody cover in African savannas. *Nature*, **438**(7069), 846–849. <https://doi.org/10.1038/nature04070>
- Schmidt, G., Jenkerson, C.B., Masek, J., Vermote, E. & Gao, F. (2013) Landsat ecosystem disturbance adaptive processing system (LEDAPS) algorithm description. In: *Open-file report (no. 2013–1057)*. U.S. Geological Survey. <https://doi.org/10.3133/ofr20131057>
- Schmidt, M., Lucas, R., Bunting, P., Verbesselt, J. & Armston, J. (2015) Multi-resolution time series imagery for forest disturbance and regrowth monitoring in Queensland, Australia. *Remote Sensing of Environment*, **158**, 156–168. <https://doi.org/10.1016/j.rse.2014.11.015>
- Schneibel, A., Frantz, D., Roder, A., Stellmes, M., Fischer, K. & Hill, J. (2017) Using annual Landsat time series for the detection of dry Forest degradation processes in south-central Angola. *Remote Sensing*, **9**(9). <https://doi.org/10.3390/rs9090905>
- Schwieder, M., Leitão, P.J., da Cunha Bustamante, M.M., Ferreira, L.G., Rabe, A. & Hostert, P. (2016) Mapping Brazilian savanna vegetation gradients with Landsat time series. *International Journal of Applied Earth Observation and Geoinformation*, **52**, 361–370. <https://doi.org/10.1016/j.jag.2016.06.019>
- Senf, C., Laštovička, J., Okujeni, A., Heurich, M. & van der Linden, S. (2020) A generalized regression-based unmixing model for mapping forest cover fractions throughout three decades of Landsat data. *Remote Sensing of Environment*, **240**, 111691. <https://doi.org/10.1016/j.rse.2020.111691>
- Settle, J.J. & Drake, N.A. (1993) Linear mixing and the estimation of ground cover proportions. *International Journal of Remote Sensing*, **14**(6), 1159–1177. <https://doi.org/10.1080/01431169308904402>
- Slootweg, S. (2016). *Move child move! Towards middle and high income for the people of the Ngorongoro district*.
- Slootweg, S. (2017). *Tourism and income growth for the Ngorongoro District population in Tanzania*. 7th European Conference on Africa Studies, Basel.
- Smit, I.P.J., Asner, G.P., Govender, N., Kennedy-Bowdoin, T., Knapp, D.E. & Jacobson, J. (2010) Effects of fire on woody vegetation structure in African savanna. *Ecological Applications*, **20**(7), 1865–1875. <https://doi.org/10.1890/09-0929.1>
- Souverijns, N., Buchhorn, M., Horion, S., Fensholt, R., Verbeeck, H., Verbesselt, J. et al. (2020) Thirty years of land cover and fraction cover changes over the Sudano-Sahel using Landsat time series. *Remote Sensing*, **12**(22), 3817. <https://doi.org/10.3390/rs12223817>
- Stevens, N., Erasmus, B.F.N., Archibald, S. & Bond, W.J. (2016) Woody encroachment over 70 years in South African savannas: overgrazing, global change or extinction

- aftershock? *Philosophical Transactions of the Royal Society B-Biological Sciences*, **371**(1703). <https://doi.org/10.1098/rstb.2015.0437>
- Stevens, N., Lehmann, C.E.R., Murphy, B.P. & Durigan, G. (2017) Savanna woody encroachment is widespread across three continents. *Global Change Biology*, **23**(1), 235–244. <https://doi.org/10.1111/gcb.13409>
- Suess, S., van der Linden, S., Okujeni, A., Griffiths, P., Leitão, P.J., Schwieder, M. et al. (2018) Characterizing 32 years of shrub cover dynamics in southern Portugal using annual Landsat composites and machine learning regression modeling. *Remote Sensing of Environment*, **219**, 353–364. <https://doi.org/10.1016/j.rse.2018.10.004>
- Swanson, L.A. (2007) *Ngorongoro conservation area: spring of life [master of environmental studies capstone projects]*. Philadelphia, PA: University of Pennsylvania.
- Symeonakis, E. & Higginbottom, T. (2014) Bush encroachment monitoring using multi-temporal Landsat data and random forests. *ISPRS Technical Commission II Symposium*, **40–42**, 29–35. <https://doi.org/10.5194/isprsarchives-XL-2-29-2014>
- Symeonakis, E., Higginbottom, T.P., Petroulaki, K. & Rabe, A. (2018) Optimisation of Savannah land cover characterisation with optical and SAR data. *Remote Sensing*, **10**(4). <https://doi.org/10.3390/rs10040499>
- TAWIRI & NCAA. (2020) *Evaluation of land cover dynamics and their management implications in the Ngorongoro Conservation Area, Tanzania*. Arusha: Tanzania Wildlife Research Institute (TAWIRI) and Ngorongoro Conservation Area Agency (NCAA).
- Teillet, P.M., Guindon, B. & Goodenough, D.G. (1982) On the slope-aspect correction of multispectral scanner data. *Canadian Journal of Remote Sensing*, **8**(2), 84–106. <https://doi.org/10.1080/07038992.1982.10855028>
- Tsalyuk, M., Kelly, M. & Getz, W.M. (2017) Improving the prediction of African savanna vegetation variables using time series of MODIS products. *ISPRS Journal of Photogrammetry and Remote Sensing*, **131**, 77–91. <https://doi.org/10.1016/j.isprsjprs.2017.07.012>
- Tucker, C.J. (1979) Red and photographic infrared linear combinations for monitoring vegetation. *Remote Sensing of Environment*, **8**(2), 127–150. [https://doi.org/10.1016/0034-4257\(79\)90013-0](https://doi.org/10.1016/0034-4257(79)90013-0)
- UNESCO. (2010) *World heritage list*. Ngorongoro Conservation Area. <https://whc.unesco.org/en/list/39/>
- Van der Linden, S., Rabe, A., Held, M., Jakimow, B., Leitão, P.J., Okujeni, A. et al. (2015) The EnMAP-box—a toolbox and application programming Interface for EnMAP data processing. *Remote Sensing*, **7**(9), 11249–11266. <https://doi.org/10.3390/rs70911249>
- Venter, Z.S., Cramer, M.D. & Hawkins, H.J. (2018) Drivers of woody plant encroachment over Africa. *Nature Communications*, **9**. <https://doi.org/10.1038/s41467-018-04616-8>
- Verbesselt, J., Hyndman, R., Newnham, G. & Culvenor, D. (2010) Detecting trend and seasonal changes in satellite image time series. *Remote Sensing of Environment*, **114**(1), 106–115. <https://doi.org/10.1016/j.rse.2009.08.014>
- Verbesselt, J., Hyndman, R., Zeileis, A. & Culvenor, D. (2010) Phenological change detection while accounting for abrupt and gradual trends in satellite image time series. *Remote Sensing of Environment*, **114**(12), 2970–2980. <https://doi.org/10.1016/j.rse.2010.08.003>
- Woodcock, C.E., Allen, R., Anderson, M., Belward, A., Bindschadler, R., Cohen, W. et al. (2008) Free access to Landsat imagery. *Science*, **320**(5879), 1011.
- Wu, L., Li, Z., Liu, X., Zhu, L., Tang, Y., Zhang, B. et al. (2020) Multi-type Forest change detection using BFAST and monthly Landsat time series for monitoring spatiotemporal dynamics of forests in subtropical wetland. *Remote Sensing*, **12**(2), 341. <https://doi.org/10.3390/rs12020341>
- Wulder, M.A., Masek, J.G., Cohen, W.B., Loveland, T.R. & Woodcock, C.E. (2012) Opening the archive: how free data has enabled the science and monitoring promise of Landsat. *Remote Sensing of Environment*, **122**, 2–10. <https://doi.org/10.1016/j.rse.2012.01.010>

Supporting Information

Additional supporting information may be found online in the Supporting Information section at the end of the article.

Figure S1 Rainfall in The Ngorongoro between January 1985 and June 2020.

Figure S2. Example of spectral data using near-infrared, green and red bands for bushland, forest, montane heath, shrubland and woodland for the year 2020.

Figure S3. Example of spectral data using SWIR, red and green bands for bushland, forest, montane heath, shrubland and woodland for the year 2020.

Figure S4. Grid used for validation.

Figure S5. Validation 2010.

Figure S6. Validation 2020.

Figure S7. Lerai Forest range: (A) Landsat imagery in December 1985; (B) Landsat imagery in February 2020; (C) CNES/Airbus in January 2020.

Table S1. Full validation statistics 2010.

Table S2. Full validation statistics 2020.